

Supporting information for

Vacuum Ultraviolet Ionization-Induced Reaction of Neutral Au₂Al₂O₃ Clusters with Methane

Jiao-Jiao Chen^{†,‡,§}, Yuan Yang^{†,‡,§}, Yan-Xia Zhao^{,†,‡}, Sheng-Gui He^{*,†,‡,§}*

[†]State Key Laboratory for Structural Chemistry of Unstable and Stable Species, Institute of Chemistry, Chinese Academy of Sciences, Beijing 100190, China

[‡]Beijing National Laboratory for Molecular Sciences, CAS Research/Education Center of Excellence in Molecular Sciences, Beijing 100190, China

[§]University of Chinese Academy of Sciences, Beijing 100049, China

*Corresponding author. E-mail address: chemzyx@iccas.ac.cn; shengguihe@iccas.ac.cn.

Table of Contents

Figure S1. DFT-calculated structural isomers of the neutral $\text{Au}_2\text{Al}_2\text{O}_3$ cluster (Page S3)

Figure S2. Additional time-of-flight (TOF) mass spectra for reactions of neutral $\text{Au}_x\text{Al}_y\text{O}_z$ clusters with CH_4 and CD_4 (Page S4)

Figure S3. Complete DFT results for VUV ionization induced reaction of neutral $\text{Au}_2\text{Al}_2\text{O}_3$ cluster with CH_4 (Page S5)

Figure S4. DFT-calculated potential-energy profile for VUV ionization of I5 to generate CH_3^\bullet (Page S6)

Figure S5. DFT-calculated structural isomers of neutral $\text{Au}_2\text{Al}_2\text{O}_4$ cluster (Page S7)

Figure S6. DFT-calculated potential-energy profile for VUV ionization induced reaction of neutral $\text{Au}_2\text{Al}_2\text{O}_4$ cluster with CH_4 (Page S8)

Figure S7. A comparison of the time-of-flight mass spectra for reactions of methane with $\text{Au}_2\text{Al}_2\text{O}_3^+$ and $\text{Au}_2\text{Al}_2\text{O}_4^+$ clusters (Pages S9-S10)

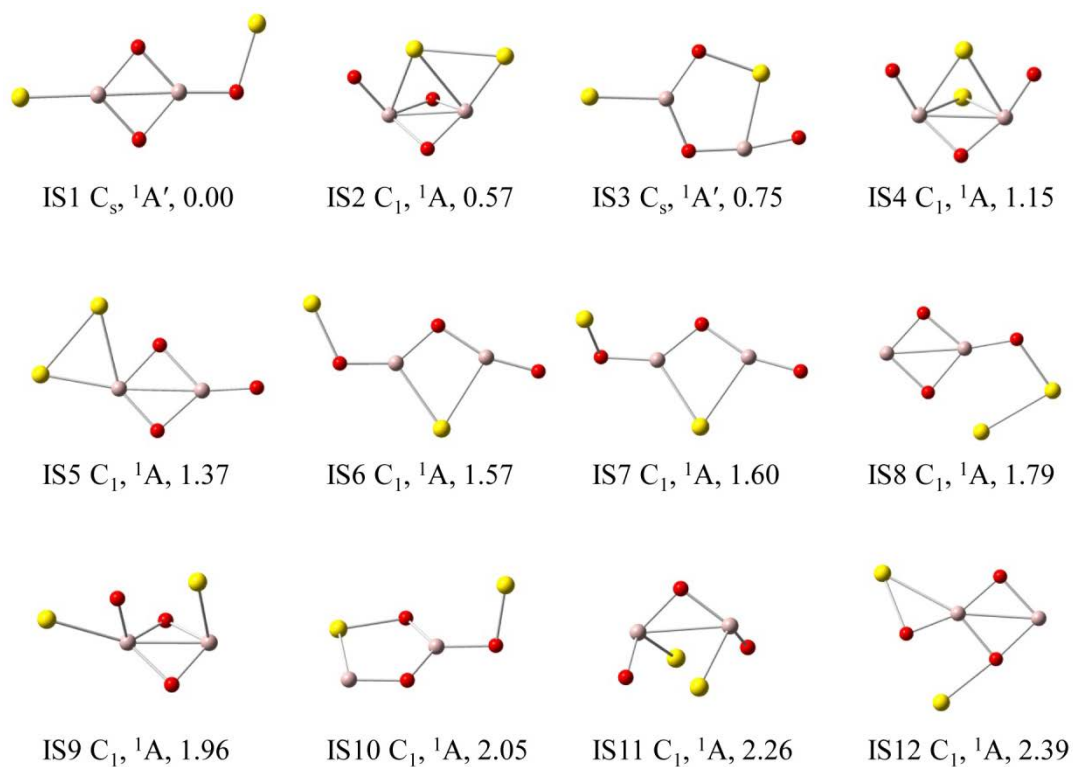


Figure S1. The DFT optimized structural isomers of neutral $Au_2Al_2O_3$ cluster. The symmetry, electronic state, and relative energies (in eV, with zero-point vibrational energy correction) are listed below each structure.

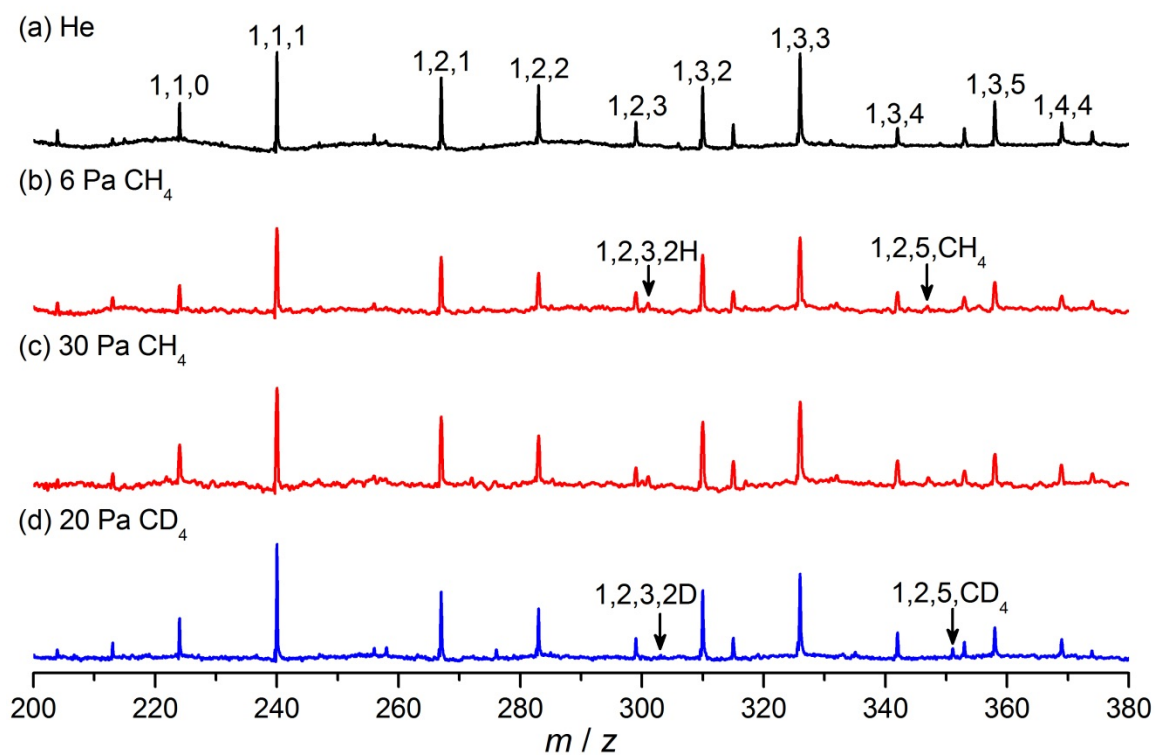


Figure S2. TOF mass spectra for the reactions of neutral Au_xAl_yO_z clusters (a) with CH₄ (b, c), and CD₄ (d). The reactant gas pressures are shown. Au_xAl_yO_z is denoted as x, y, z and Au_xAl_yO_zX is denoted as x, y, z, X ($X = \text{H}, \text{D}, \text{CH}_4, \text{CD}_4$).

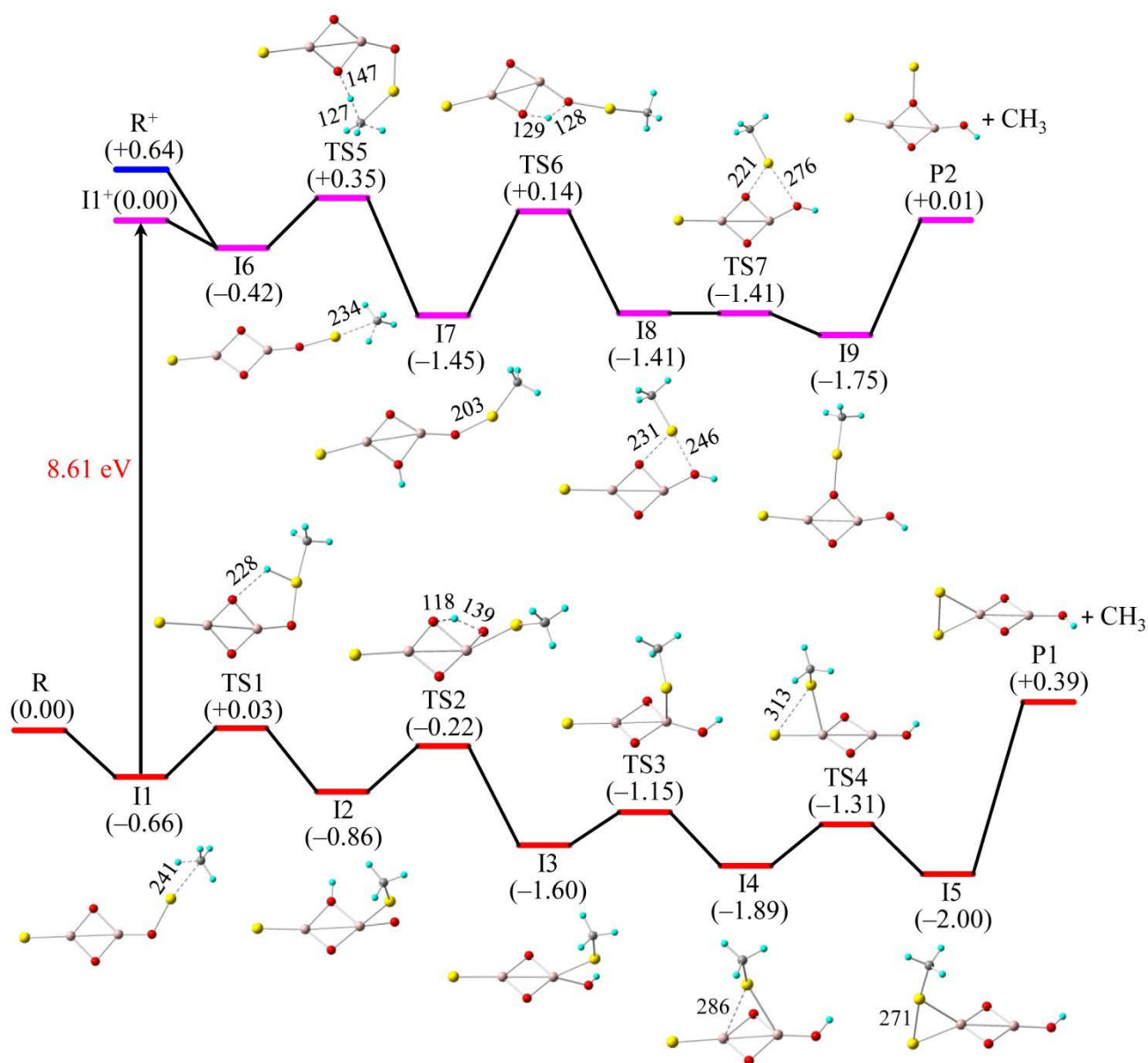


Figure S3. DFT-calculated potential-energy profile for VUV ionization induced reaction of neutral $\text{Au}_2\text{Al}_2\text{O}_3$ cluster with CH_4 (R). The structures of the intermediates (I1–I9), transition states (TS1–TS7), and products (P1 and P2) are shown. The relative energies (eV) of the reaction intermediates (I1–I5), transition states (TS1–TS4), and products (P1) are with respect to the separated reactants (R). The relative energies (eV) of the separated reactants (R^+ : $\text{Au}_2\text{Al}_2\text{O}_3^+$ and CH_4), reaction intermediates (I6–I9), transition states (TS5–TS7), and products (P2) are with respect to I1^+ . The vertical ionization energy of I1 and the bond lengths (in pm) are also shown.

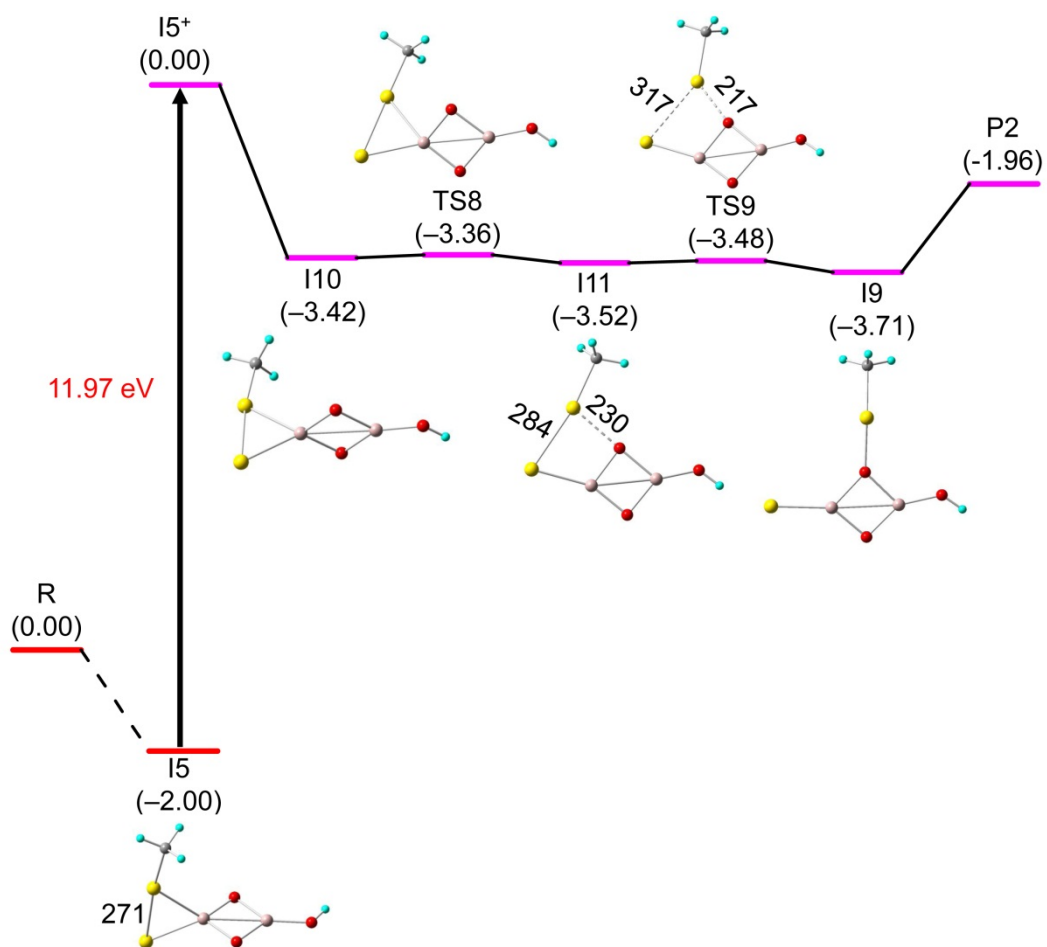


Figure S4. DFT-calculated potential-energy profile for VUV ionization of I5 to generate CH₃[•]. The relative energies (eV) of reaction intermediates (I9–I11), transition states (TS8 and TS9), and products (P2) are with respect to I5⁺. The vertical ionization energy of I5 and the bond lengths (in pm) are also shown.

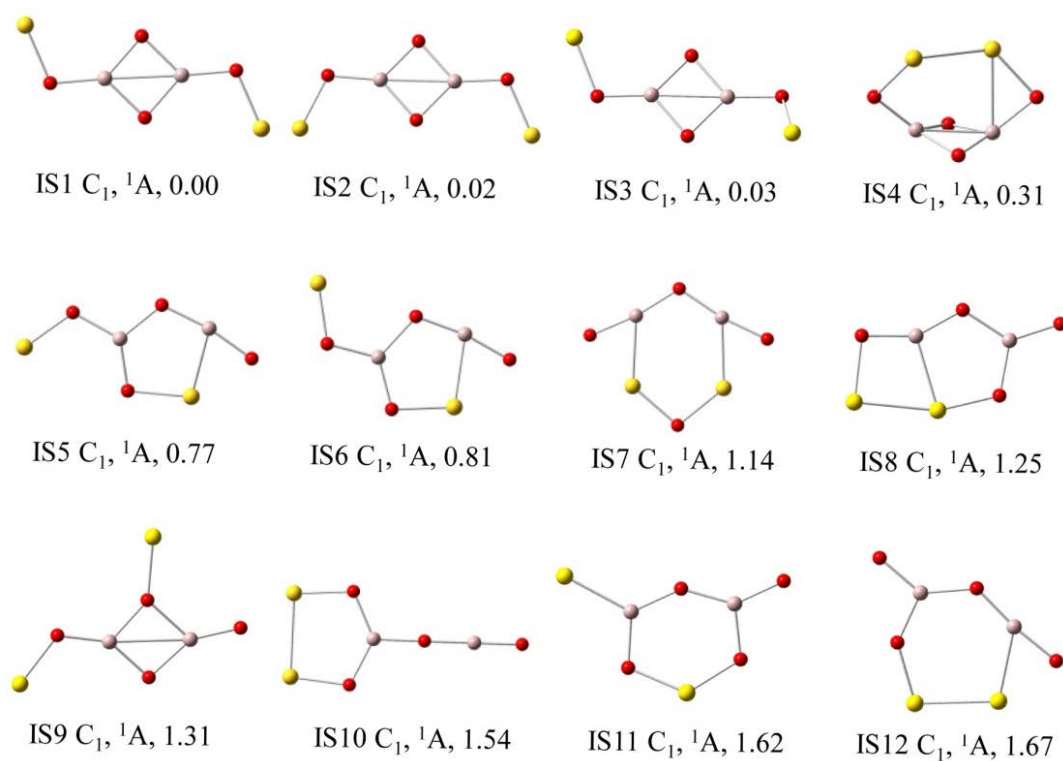


Figure S5. The DFT optimized structural isomers of neutral $Au_2Al_2O_4$ cluster. The symmetry, electronic state, and relative energies (in eV, with zero-point vibrational energy correction) are listed below each structure.

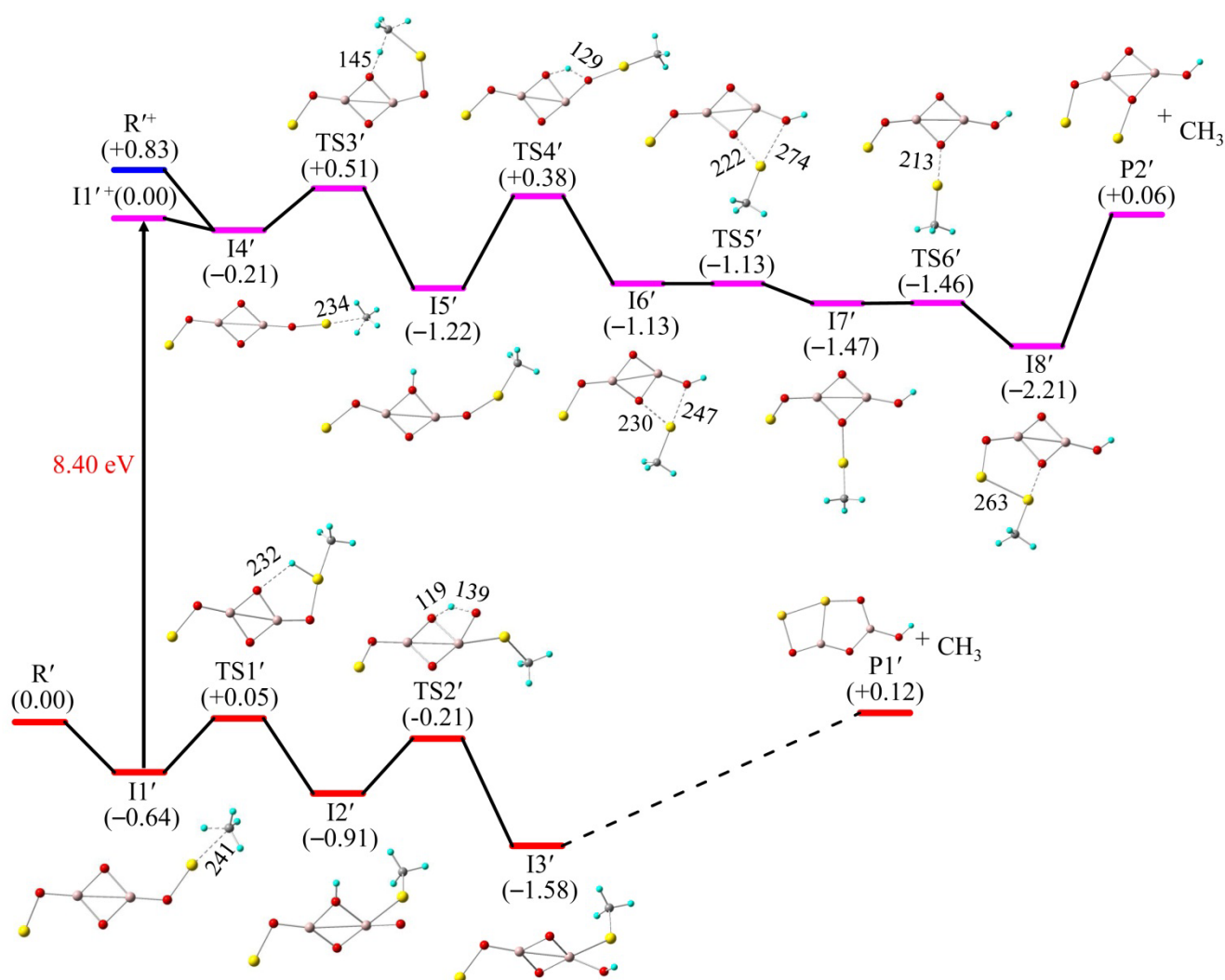


Figure S6. DFT-calculated potential-energy profile for VUV ionization induced reaction of neutral $\text{Au}_2\text{Al}_2\text{O}_4$ cluster with CH_4 (R'). The structures of the intermediates ($\text{I1}'$ – $\text{I8}'$), transition states ($\text{TS1}'$ – $\text{TS6}'$), and products ($\text{P1}'$ and $\text{P2}'$) are shown. The relative energies (eV) of the reaction intermediates ($\text{I1}'$ – $\text{I3}'$), transition states ($\text{TS1}'$ – $\text{TS2}'$), and products ($\text{P1}'$) are with respect to the separated reactants (R'). The relative energies (eV) of the separated reactants (R'^+ : $\text{Au}_2\text{Al}_2\text{O}_4^+$ and CH_4), reaction intermediates ($\text{I4}'$ – $\text{I8}'$), transition states ($\text{TS3}'$ – $\text{TS6}'$), and products ($\text{P2}'$) are with respect to $\text{I1}'^+$. The vertical ionization energy of I1 and the bond lengths (in pm) are also shown.

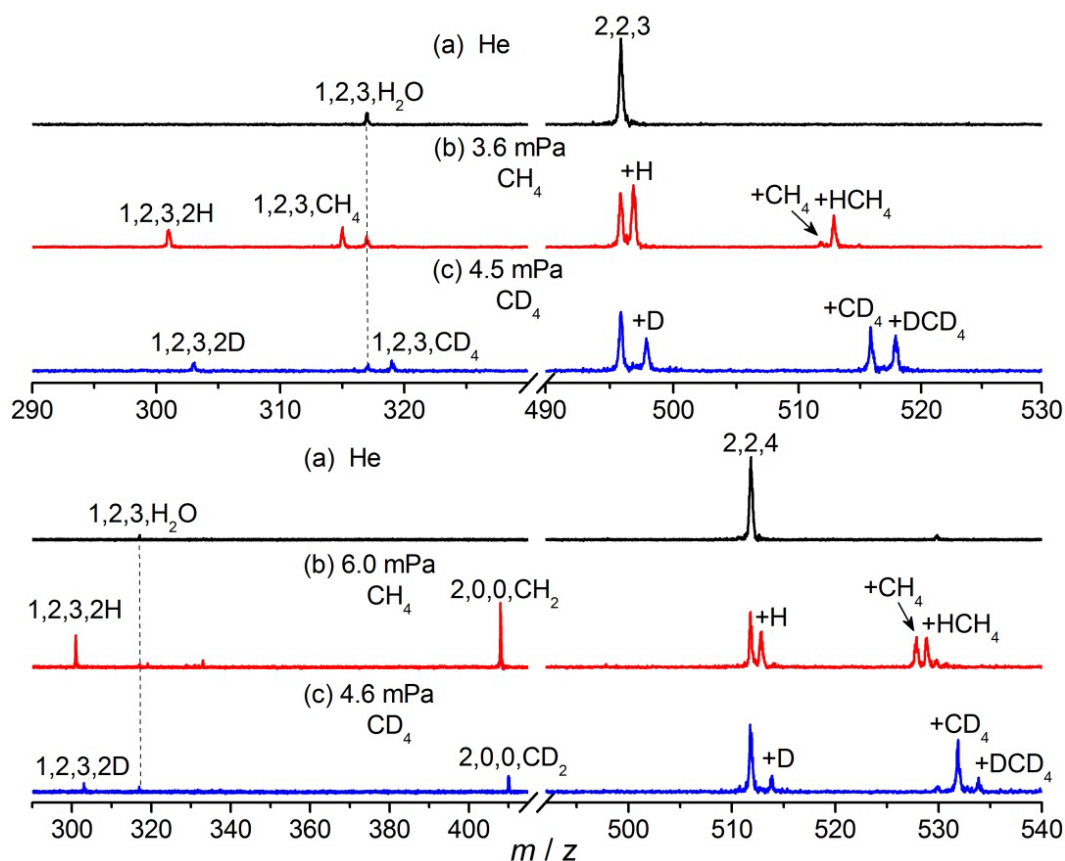
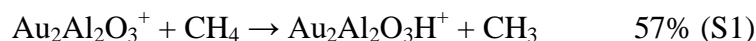
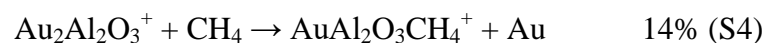
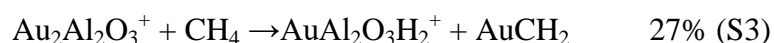
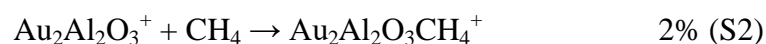


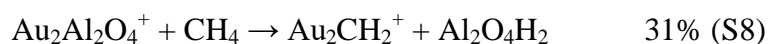
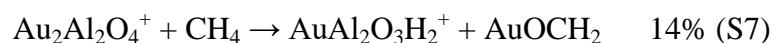
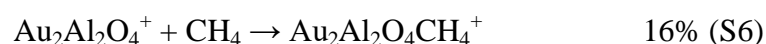
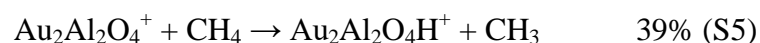
Figure S7. The TOF mass spectra for the reactions of mass-selected $\text{Au}_2\text{Al}_2\text{O}_3^+$ and $\text{Au}_2\text{Al}_2\text{O}_4^+$ clusters (a) with CH_4 (b) and CD_4 (c) in an ion trap reactor for about 1.9 ms. The reactant gas pressures are shown. $\text{Au}_x\text{Al}_y\text{O}_z^+$ is denoted as x, y, z and $\text{Au}_x\text{Al}_y\text{O}_z\text{X}^+$ is denoted as x, y, z, X ($\text{X} = \text{H}, \text{D}, \text{CH}_4, \text{CD}_4$, etc.). The label $+ \text{X}$ denotes $\text{Au}_2\text{Al}_2\text{O}_{3,4}\text{X}^+$ ($\text{X} = \text{H}, \text{D}, \text{CH}_4, \text{CD}_4$, etc.).

Figure S7 shows the time-of-flight mass spectra for the interactions of mass-selected $\text{Au}_2\text{Al}_2\text{O}_3^+$ ($m/z = 496$) and $\text{Au}_2\text{Al}_2\text{O}_4^+$ ($m/z = 512$) clusters with CH_4 and CD_4 . The experimental details of $\text{Au}_2\text{Al}_2\text{O}_4^+$ cluster reaction system are similar to that of $\text{Au}_2\text{Al}_2\text{O}_3^+$.¹ It is noticeable that the both of the two clusters can react with a trace amount of H_2O impurity in the gas-handling system to generate $\text{AuAl}_2\text{O}_3\text{H}_2\text{O}^+$ ($\text{Au}_2\text{Al}_2\text{O}_3^+ + \text{H}_2\text{O} \rightarrow \text{AuAl}_2\text{O}_3\text{H}_2\text{O}^+ + \text{Au}$ and $\text{Au}_2\text{Al}_2\text{O}_4^+ + \text{H}_2\text{O} \rightarrow \text{AuAl}_2\text{O}_3\text{H}_2\text{O}^+ + \text{AuO}$). The product peaks assigned as $\text{Au}_2\text{Al}_2\text{O}_3\text{H}^+$, $\text{Au}_2\text{Al}_2\text{O}_3\text{CH}_4^+$, $\text{AuAl}_2\text{O}_3\text{H}_2^+$, and $\text{AuAl}_2\text{O}_3\text{CH}_4^+$ were observed for the reaction of $\text{Au}_2\text{Al}_2\text{O}_3^+$ cluster with CH_4 ,¹ suggesting the following reaction channels [Eq.(S1)-(S4)]:





Similarly, the product peaks assigned as $\text{Au}_2\text{Al}_2\text{O}_4\text{H}^+$, $\text{Au}_2\text{Al}_2\text{O}_4\text{CH}_4^+$, $\text{AuAl}_2\text{O}_3\text{H}_2^+$, and AuCH_2^+ were observed for the reaction of $\text{Au}_2\text{Al}_2\text{O}_4^+$ cluster with CH_4 , as shown below [Eq.(S5)-(S8)]:



It is clear that the branching ratio of association channel (16%) for generation of $\text{Au}_2\text{Al}_2\text{O}_4\text{CH}_4^+$ is larger than that (2%) of $\text{Au}_2\text{Al}_2\text{O}_3\text{CH}_4^+$.

References

(1) Zhou, X.-H.; Li, Z.-Y.; Jiang, L.-X.; He, S.-G.; Ma, T.-M. Methane Activation Mediated by Dual Gold Atoms Doped in Aluminium Oxide Cluster Cations $\text{Au}_2\text{Al}_2\text{O}_3^+$. *Chemistryselect* **2017**, 2, 991-996.